Hindawi
Advances in Civil Engineering
Volume 2019, Article ID 3069029, 11 pages
https://doi.org/10.1155/2019/3069029

Research Article

Microcrack Growth Properties of Granite under Ultrasonic High-Frequency Excitation

Dajun Zhao[1,2], **Shulei Zhang**[1,2] **and Meiyan Wang**[1,2]

[1]*College of Construction Engineering, Jilin University, Changchun 130026, China*
[2]*Key Laboratory of Drilling Technology in Complex Conditions of Ministry of Land and Resources of the People's Republic of China, No. 938 Ximinzhu Street, Changchun 130026, China*

Correspondence should be addressed to Shulei Zhang; slzhang16@mails.jlu.edu.cn

Received 27 January 2019; Revised 10 April 2019; Accepted 19 May 2019; Published 18 June 2019

Academic Editor: Abdul Aziz bin Abdul Samad

The failure of most rock materials is essentially a process of crack initiation and propagation. It is of great significance to study the microcrack growth characteristics of granite under ultrasonic high-frequency excitation for understanding the failure mechanism of rock under ultrasonic vibration. In this paper, the experimental and numerical simulation methods are used to study the propagation characteristics of rock cracks under ultrasonic vibration. Scanning electron microscopy (SEM) was used to observe the growth of microcracks in granite samples after ultrasonic vibration for 0 min, 2 min, and 4 min. A discrete element software PFC^{2D} was used to simulate and solve the cracking mechanism of rock cracks under ultrasonic vibration. Also, it is found that the action of ultrasonic vibration can effectively promote the development of microcracks in the granite samples. The main three cracks causing the failure of quartz under the ultrasonic high frequency are intragranular cracks, transgranular cracks, and grain boundary cracks. The breakage of transgranular cracks usually contributes a shell-like fracture, that is, a regular curved surface with a concentric circular pattern appears on the fracture surface, which is a typical quartz brittle fracture mode. In addition, the feldspar grain failure is mainly caused by intragranular crack and transgranular crack. Microcracks are wavy expansion in feldspar grain. Mica failure is mainly caused by grain boundary crack, and the effect of lamellar cleavage on the failure of mica is significant. Moreover, it is also found that the mechanism of microcrack propagation is tensile failure. The failure of feldspar grains is mainly contributed to the failure of granite.

1. Introduction

Using ultrasonic vibration technology to break hard rock is a new method in the field of geological exploration [1]. Vibration can promote the development of cracks, reduce the strength, and cause damage to the rock. The instability and failure of rocks is closely related to the initiation and propagation of microcracks that are induced by cyclic vibration loads [2]. Propagation of microcracks inside the rock is determined by the external load and the internal mesostructure. Most rocks are heterogeneous materials that contain a variety of rock-forming minerals and a large number of microdefects. Granite can be used as a representative of hard rock because it is a common rock in the field of geological exploration. Therefore, understanding the microcrack propagation characteristics of granite under ultrasonic vibration is essential for understanding the mechanism of breaking hard rock under ultrasonic vibration.

Over the past few years, considerable efforts have been made to investigate the failure mechanics of intact rocks under low-frequency cyclic vibration loading. Al-Shayea [3] reported that the dynamic elastic modulus and Poisson's ratio during unloading under cyclic loading are slightly higher than those during loading. Ray et al. [4] concluded that the failure strength and elastic modulus of Chunar sandstone under cyclic stress decrease with the increase of strain rate, and the uniaxial compressive strength decreases

with the increase of loading period. Bagde and Petroš [5, 6] performed a cyclic loading test on the rock to study the relationship between loading amplitude and frequency and fatigue strength and deformation behavior. It is found that the dynamic axial stiffness of the rock decreases with increasing loading frequency and amplitude. The fatigue phenomenon developed in the specimens under dynamic cyclic loading and the axial stiffness decreased due to fatiguing. Liu et al. [7] established a damage constitutive model based on energy dissipation for intact rock subjected to cyclic loading. The fatigue tests carried out by Le et al. indicate that there is a small-crack growth regime at the beginning stage of cyclic loading, where the growth rate decreases as the crack initiates from the notch tip [8]. Numerical studies conducted by Ghamgosar and Erarslan show that the maximum principal stress (tensile stress) of fracture process zone under static load is higher than the induced tensile stress under cyclic loading [9].

Meanwhile, a few scholars and institutes are engaged in the research of rock breaking under ultrasonic vibration. Wiercigroch et al. [10] performed an ultrasonic drilling rock test indoors. It is found that an introduction of high-frequency axial vibration significantly enhances drilling rates compared to the traditional rotary type method and the material removal rate (MRR) as a function of static load has at least one maximum. Fernando et al. [1] selected basalt, marble, and travertine as the research objects to carry out ultrasonic drilling test. The results indicate that rotary ultrasonic machining can drill holes of high quality on rocks of different hardness with a much lower cutting force and at a penetration rate of approximately three times faster than percussive. In our previous study, CT was used to detect granite after ultrasonic vibration. It was found that the optimum preloading value was 400 N when rock was broken by ultrasonic vibration. However, limited to the accuracy of CT, the shape of cracks cannot be observed [11]. At present, the research on rock breaking technology by ultrasonic vibration is still in the laboratory stage. Few were reported about the mechanism of microcrack propagation inside rock under the action of ultrasonic high-frequency excitation from a microcosmic point of view. The propagation mechanism of rock cracks under ultrasonic vibration still remains unclear. The microcracking inside the rock can be investigated using numerical simulation software [12–14] or scanning electron microscopy [15–17]. The discrete element software PFC^{2D} has been widely used in numerical simulation of crack propagation characteristics in rock under various loads. It can reveal the failure mechanism of geomaterials from the perspective of micromechanics, reproduce the process of crack initiation and evolution, and make up for the defects in the laboratory test that it is difficult to capture the dynamic crack propagation process [18, 19].

In this study, the discrete element software PFC^{2D}, ultrasonic vibration tests, and scanning electron microscopy are used to investigate the microcrack propagation characteristics of granite under high-frequency ultrasonic excitation. The electron microscope pictures of microcrack in the rock-forming minerals on the surface of granite samples under various ultrasound high-frequency excitation time are collected. Crack orientation and the curve of crack changing with time step are obtained by numerical simulation. Through the analysis of the SEM images and numerical simulation results, the microcrack growth characteristics and the crack propagation mechanism are investigated.

2. Numerical Simulation and Experiment

2.1. Numerical Model. PFC, the discrete element numerical simulation software based on particle flow method, can simulate the fracture damage mechanism of rock materials from a mesomechanical point of view, reproduce the process of dynamic crack propagation, and make up for the defects of difficult to capture crack dynamic expansion information in indoor experiments [14]. It has been successfully used by many scholars to study the internal crack propagation behavior of granite under external load [19, 20]. In this study, the PFC^{2D} software is used to establish a two-dimensional heterogeneous granite model to solve the cracking mechanism of rock cracks under ultrasonic vibration. In the process of modeling, the loading of ultrasonic vibration load is realized by applying a sinusoidal velocity to the wall on the top of the rock model. Set the wall speed at the bottom of the rock model to 0 for the purpose of fixing the bottom of the rock model. The rock model and boundary conditions are shown in Figure 1.

The ultrasonic vibration displacement load U is as follows:

$$U = A\sin(\omega t), \tag{1}$$

where A is the maximum amplitude of the ultrasonic vibration output and ω is the frequency of ultrasonic vibration.

The velocity load F applied to the wall can be obtained by deriving formula (1), as follows:

$$F = A\omega\cos(\omega t). \tag{2}$$

The amplitude "$A = 22\,\mu$m," the angular velocity "$\omega = 2\pi f$," the frequency of the ultrasonic vibration $f = 40000$ Hz, and the load finally applied to the rock model are shown in the following equation:

$$F = 1.76\pi\cos(80000\pi t). \tag{3}$$

The mesomechanical parameters of the rock model are shown in Table 1.

2.2. Ultrasonic Vibration Loading Test

2.2.1. Rock Sample. The test samples were medium-grained granites originated from the southern Zhangguangcai Ling area located in the northeastern area of Jilin Province. Its main mineral compositions include quartz (0.5–2.5 mm, 20–30%), feldspar (0.6–3.0 mm, 60–70%), mica (0.5–2.0 mm, 5–7%), and other minerals (<1%) [21]. The mechanical parameters of major rock-forming mineral including quartz, feldspar, mica are shown in Table 2. Due to the limitations of S-4800FESEM, the specific requirement of samples is the 9 mm × 9 mm × 9 mm. Figure 2 shows the rock

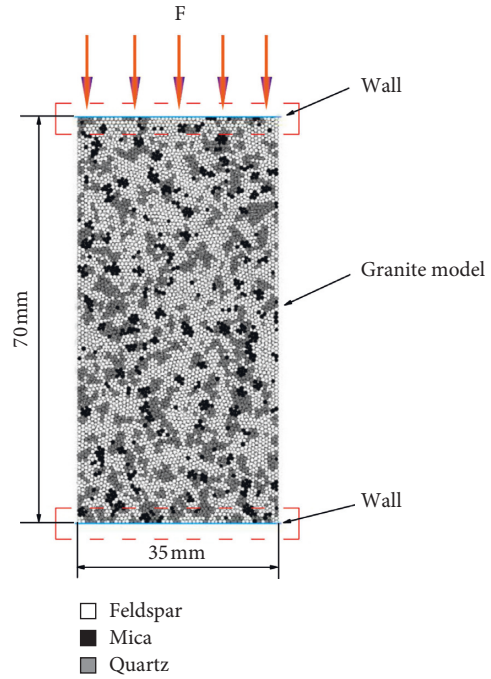

Figure 1: Rock model and boundary conditions.

Table 1: Mesomechanical parameters of rock model.

Name	Density ρ (g/cm^3)	Effective modulus of particle, E_c (GPa)	Ratio of normal to shear stiffness of the particle k_n/k_s	Particle friction coefficient μ	Parallel bond tensile strength $\overline{\sigma}_c$ (MPa)	Parallel bonding cohesion $\overline{c}$ (MPa)	Parallel bond friction angle $\overline{\phi}$ (°)	Normal stiffness per unit area of smooth stiffness model $\overline{k}_n$ (N·m^{-3})	Shear stiffness per unit area of smooth stiffness model $\overline{k}_s$ (N·m^{-3})
Mica	2900	20	2.5	0.5	300	600	20	2.19e^{13}	8.78e^{12}
Feldspar	2800	40	2.5	0.5	400	800	30	4.65e^{13}	1.86e^{13}
Quartz	3000	60	2.5	0.5	500	1000	40	7.90e^{13}	3.16e^{13}

Table 2: The mechanical parameters of major rock-forming mineral [22, 23].

Rock-forming minerals	Young's modulus (GPa)	Poisson's ratio	Compressive strength (MPa)	Tensile strength (MPa)	Cohesion (MPa)
Quartz	90	0.17	100	14	55
Feldspar	69.0	0.28	90	11	11
Mica	40	0.27	60	7	30

Figure 2: Rock samples.

sample in this study. Also, its flatness and parallelism of any two planes are required to be higher than 5/1000.

2.2.2. Experimental Devices. CHSX5640, a rock sample processing equipment produced by Taizhou Chen Hong Computer Numerical Control (CNC) Equipment Manufacturing Co., Ltd., is used in this study (Figure 3). The main technical parameters of CHSX5640 are as follows: X, Y table surface flatness measured in the length of 1000 is 0.04, table positioning accuracy measured in the length of 500 is 0.02, perpendicular to the X-axis and Y-axis of the table is 0.01/100, parallel to the direction of movement of the X and Y of the

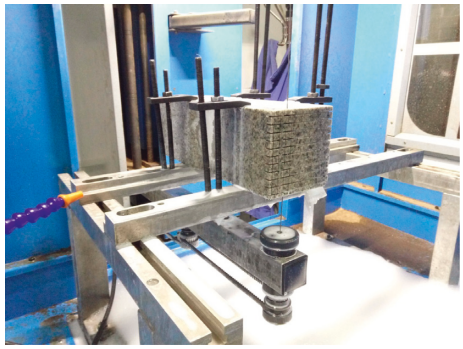

Figure 3: Rock sample processing.

sand line and the bow frame is 0.01/100, and X, Y movement straightness measured length of 500 is 0.015. Its parameters can ensure that the processed cube samples could meet the test requirements. This study used ultrasonic high-frequency excitation vibration test equipment (Figure 4) as a ultrasonic vibration test platform consisting of ultrasonic drive power supply, bracket, ultrasonic transducer, timer, weight, and stage composition. This ultrasonic generator has a 40 KHz vibration frequency and a 220 V ultrasonic generator driving voltage with power arranging at 0–800 W. Its maximum amplitude can reach at 22 μm. Figure 5 shows S-4800FESEM SEM, one microcrack observation device produced by Hitachi. The scanning electron microscope has a 1.4 nm electronic resolution (1 kV, deceleration mode), an acceleration voltage ranging at 0.5–30 kV (0.1 kV/step, variable), and a magnification at 20–800000. Its electron gun adapts field emission electron source.

2.2.3. Test Scheme. In this study, granite is processed into cubic by the diamond cutting machine, and the size of cubic is 9 mm × 9 mm × 9 mm. The samples were washed by anhydrous ethanol and dried in the oven at 80°C. In order to ensure that the spectrometer can distinguish different rock minerals, the sample surface is not treated, and the sample is connected with the holder by a conductive adhesive tape, so as to avoid the electronics accumulation happening on the observing interface. In the ambient temperature (25°C), uniaxial vibrations of the rock samples were carried out for 0 min, 2 min, and 4 min by ultrasonic high-frequency excitation experimental device. The test parameters can be seen in Table 3. Also, the crack propagation on the same side of the rock specimen after different loading time was observed by SEM (the loading method and the surface of the sample are shown in Figure 6; the flowchart of the whole test is shown in Figure 7).

3. Results and Discussion

Gao et al. presented that the macroscopic failure of rock is a gradual process, which is caused by the germination, expansion, evolution, and coalescence of its internal microcracks [24]. Microcracking is highly dependent on the mineralogy, fabric, and microstructure of a given rock

Figure 4: Ultrasonic high-frequency excitation experimental device.

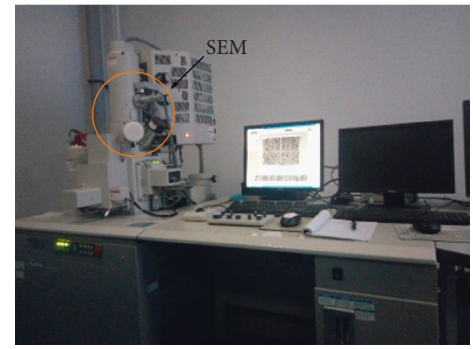

Figure 5: Crack observation equipment.

Table 3: Vibration parameters.

Excitation frequency (kHz)	Amplitude (μm)	Static load (N)	Power (W)
40	22	100	800

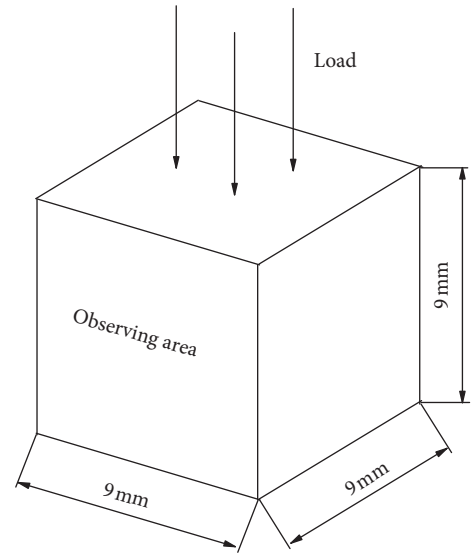

Figure 6: Schematic diagram of sample loading and observation.

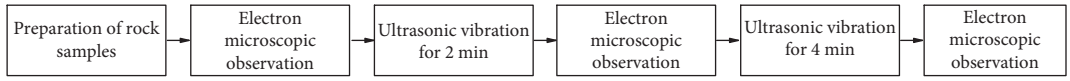

Figure 7: Test flowchart.

type [25–27]. Granite contains a variety of rock-forming minerals and contains many original defects. Therefore, the development of cracks related to different rock-forming minerals under ultrasonic vibration and the original defects inside granite are given in the following experimental results.

3.1. Microcracks. The crack surface information of the granite sample was collected first before the uniaxial ultrasonic high-frequency excitation test. The original micropores (3,000 times), microcavities (20,000 times), and microcracks (5,000 times) in the granite are revealed in Figures 8(a)–8(c), respectively. The means of "3,000 times," "20,000 times," and "5,000 times" are multiples of the electron microscope magnification. Both micropores and microcavities are almost distributed in feldspar grains. Quartz grains contain more microcracks than feldspar and mica grains. Microcracks in rock-forming minerals randomly distribute in disorder.

3.2. Quartz. Figure 9 illustrates the expansion of the microcracks in the quartz grains magnified 1000 times corresponding to 0 (Figure 9(a)), 2 (Figure 9(b)), and 4 (Figure 9(c)) minutes of ultrasonic high-frequency excitation. The main three cracks causing the failure of quartz under the ultrasonic high frequency are intragranular cracks, transgranular cracks, and grain boundary cracks. The breakage of transgranular cracks usually contributes a shell-like fracture, that is, a regular curved surface with a concentric circular pattern appears on the fracture surface, which is a typical quartz brittle fracture mode. The grain boundary cracks mainly extend along the boundaries of quartz-feldspar and quartz-mica. In contrast to Figure 8, it can be found that with the enhancement of high-frequency ultrasonic excitation time, the microcracks inside the quartz grains are expanding.

3.3. Feldspar. Intragranular cracks and transgranular cracks cause the failure of feldspar under the ultrasonic high frequency. The development of microcracks in feldspar grains (including the number of cracks and the width of crack propagation) is better than that of quartz grains. Due to the effect of vertical joints existing in feldspar, microcracks expanded wavily, which is shown in Figure 10 (18,000 times). Both Figures 10(b) and 10(c) (magnification of 10,000) show the change of microcracks in feldspar at 2 and 4 min of ultrasonic high-frequency excitation. It can be found that with the increase of ultrasonic high-frequency excitation time, the width does not increase when reaching a certain value index and the crack mainly extends along the length direction.

3.4. Mica. Due to its unique layered cleavage, mica is easy to be recognized by scanning electron microscopy. Figure 11 shows the expansion of the microcracks in the mica grains magnified 1000 times corresponding to 0, 2, and 4 minutes of ultrasonic high-frequency excitation. Comparing with quartz grains and feldspar grains, the main kind of crack causing the failure of quartz under the ultrasonic high frequency is grain boundary crack (as shown in red mark in Figure 11(b)), which includes quartz-mica grain boundary crack and feldspar-mica grain boundary crack. The lamellar cleavage (as shown in Figure 11(c) in green mark) has significant effect on the crack propagation.

3.5. Macroscopic Destruction of Granite. The ultrasonic high-frequency vibration can effectively promote the germination of new microcracks and the propagation and coalescence of the original microcrack in granite sample and finally form macroscopic cracks leading to the failure of the rock, as shown in Figure 12 (the magnification is 30 times). The direction of macroscopic crack that causes the failure of granite sample is parallel to the direction of the ultrasonic high-frequency excitation, as shown in Figure 13.

3.6. Discussion. Microcracking is highly dependent on the mineralogy, fabric, and microstructure of a given rock type [25–27]. Therefore microtextural variations are essential for understanding variation in strength and failure behavior of rocks [26]. The extension path of rock internal cracks under low-frequency loads has been reported by several researchers. For example, Swan [28] observed the crack path of subcritical crack growth in westerly granite. It was found that the higher the crack growth rate, the higher the percentage of transgranular cracks in quartz, plagioclase, and biotite. Kudo et al. [29] observed the crack path in granite and studied the interaction between the crack path and the mineral particles. Quartz particles play an important role as obstacles; feldspar particles can change the direction of the crack path due to their cleavage plane; biotite particles have a significant effect on the crack path, even if its composition ratio is very small. Erarslan [30] believes that the main difference from cyclically loaded specimens compared to static cracking is that intragranular cracks are formed due to particle breakage under cyclic loading, while smooth and bright cracks along the cleavage plane are formed under static loading. However, the frequency of the cyclic load involved in the above study is much lower than the frequency of the ultrasonic vibration. The crack path under ultrasonic vibration is still unclear.

Figures 8–10 illustrate the crack growth modes of different rock-forming minerals within the rock under high-frequency ultrasonic excitation. Three types of cracks are developed in granite samples after ultrasonic vibration. This

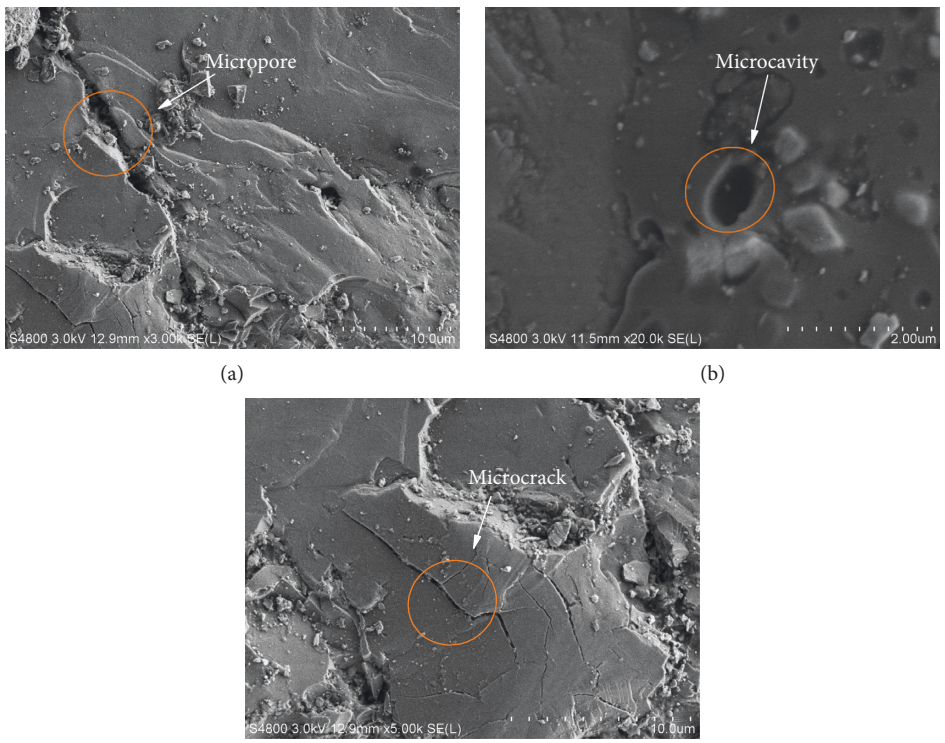

Figure 8: The original microdefects.

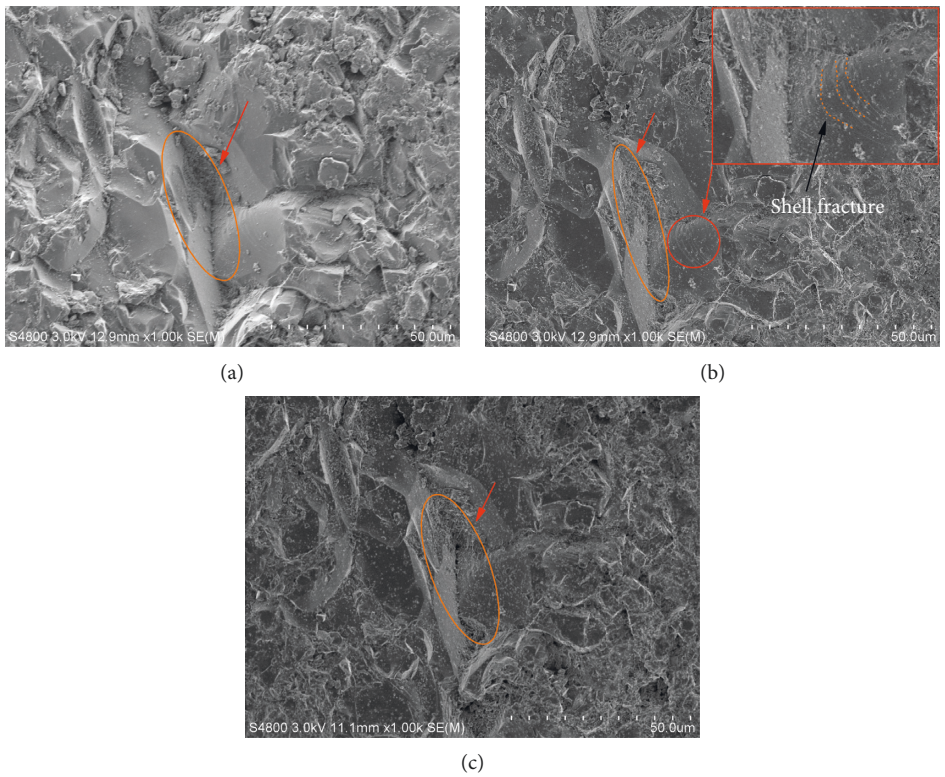

Figure 9: Quartz crack propagation graph. (a) 0 min. (b) 2 min. (c) 4 min.

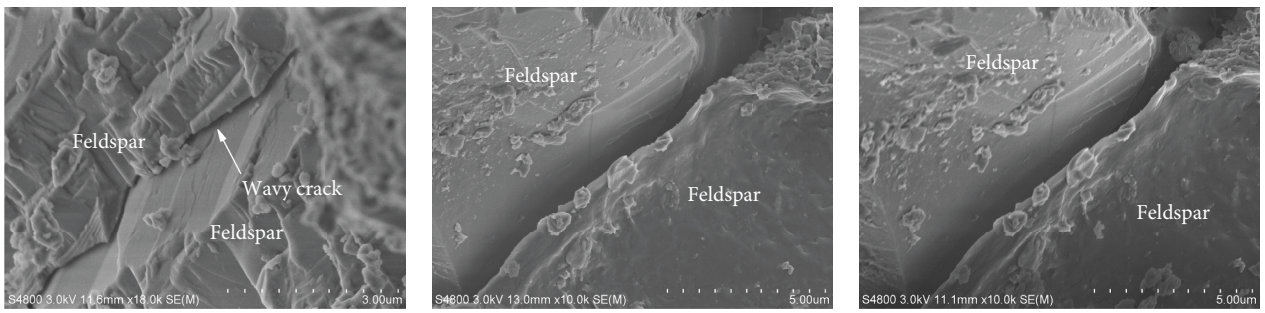

(a) (b) (c)

Figure 10: Feldspar crack propagation graph.

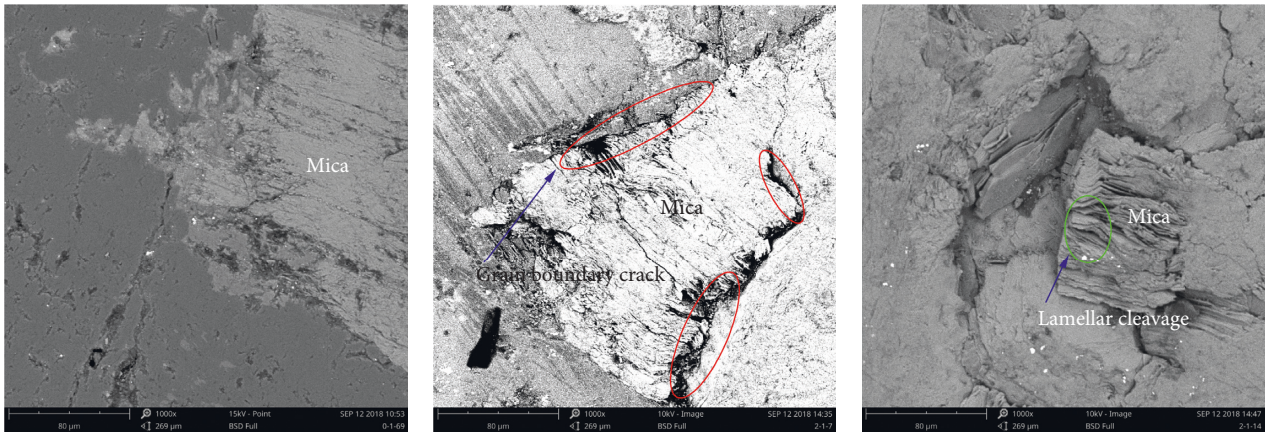

(a) (b) (c)

Figure 11: Mica crack propagation graph. (a) 0 min. (b) 2 min. (c) 4 min.

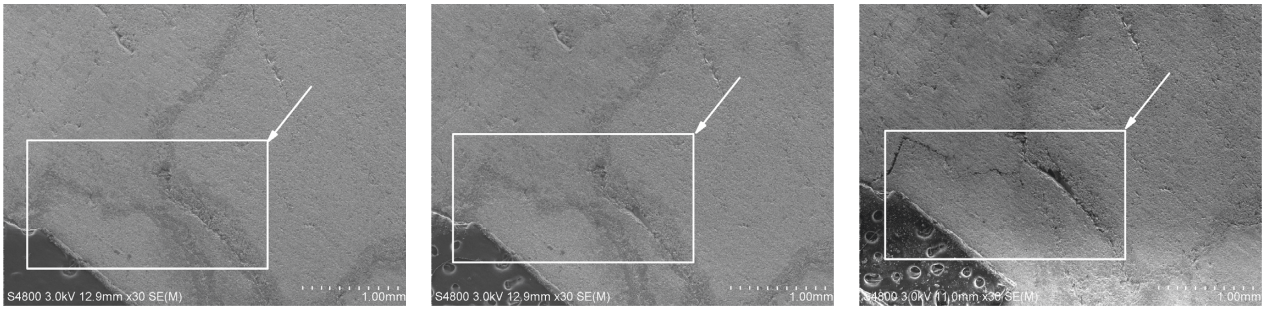

(a) (b) (c)

Figure 12: Crack evolution process. (a) 0 min. (b) 2 min. (c) 4 min.

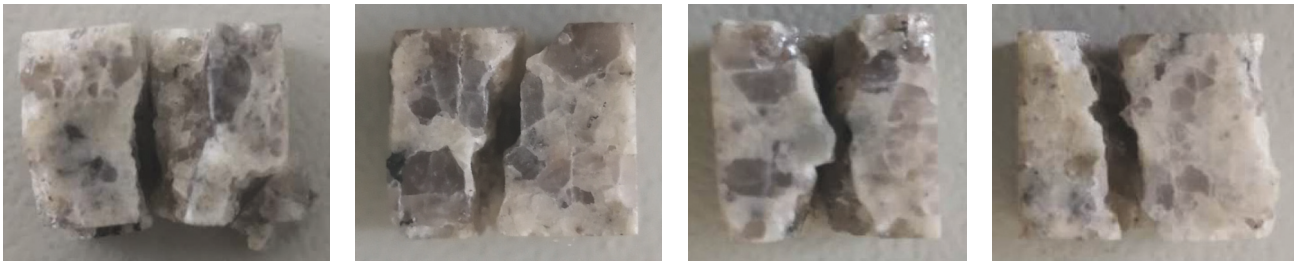

(a) (b) (c) (d)

Figure 13: Fracture morphology of the samples.

crack propagation is influenced by the heterogeneity of granite components due to different responses under repeated stresses.

Intragranular cracks, transgranular crack, and grain boundary crack are the main types of cracks that cause the failure of quartz grain. The main types of cracks that cause the feldspar failure are intragranular cracks and transgranular cracks. The main types of cracks that cause mica failure are grain boundary cracks (including quartz-mica and feldspar-mica grain boundary cracks). This difference between quartz, mica, and feldspar reflects their inherently different mechanical properties and physical structure.

Under the action of ultrasonic high-frequency excitation, the micropores, microcavities, and microcracks in granite will cause stress concentration; the difference both the mechanical parameters of the rock-forming minerals (Table 1) and the cleavage planes contained in the rock-forming minerals can also lead to differences in the degree of microcrack expansion and crack morphology. Among the three main rock-forming minerals, Young's modulus of the quartz grains is the largest, that is, the quartz has the largest stiffness, which is also the reason of the shell-like fracture appearing in the microcracks of quartz grains and showing typical brittle fracture. The mica in the granite is scattered between the quartz grains and the feldspar grains. The differences of elastic modulus of mica, quartz, and feldspar are known to be huge, and among them, Young' modulus of mica is the smallest. Under the action of ultrasonic high-frequency excitation, these differences of elastic modulus will cause huge differences of elastic deformation of mica, quartz, and feldspar and ultimately result in local stress concentration. Since the bonding strength between mica and quartz is weak as well as between micaand feldspar, grain boundary cracks are more likely to occur in the boundary of mica. Young's modulus of feldspar is smaller than that of quartz, but the feldspar stiffness is also very large. The vertical joints existing in feldspar are the cause of the wave-like expansion of fissures in the feldspar and the reason why the microcracks are easier to expand inside the feldspar than in the quartz. Due to the large amount of feldspar in granite, the failure of feldspar under ultrasonic high-frequency excitation is the main reason of granite failure.

4. Analysis of Crack Propagation Mechanism under Ultrasonic High-Frequency Excitation

Figure 14 shows the crack initiation of granite under ultrasonic vibration. The left side of Figure 14 is the label column, the middle is the granite sample, and the right side is the development of the crack. According to the label on the left side of Figure 14, there are four cracks in the rock model, including parallel bond tensile cracking cracks (green, crackpb_tension), smooth joint tensile cracking cracks (blue, cracksj_tension), parallel bond shear cracks (cyan, crack_pb_shear), and smooth joint shear cracks (red, crack_sj_shear). Because the smooth joint model is used to simulate the bond mechanics relationship between grains in

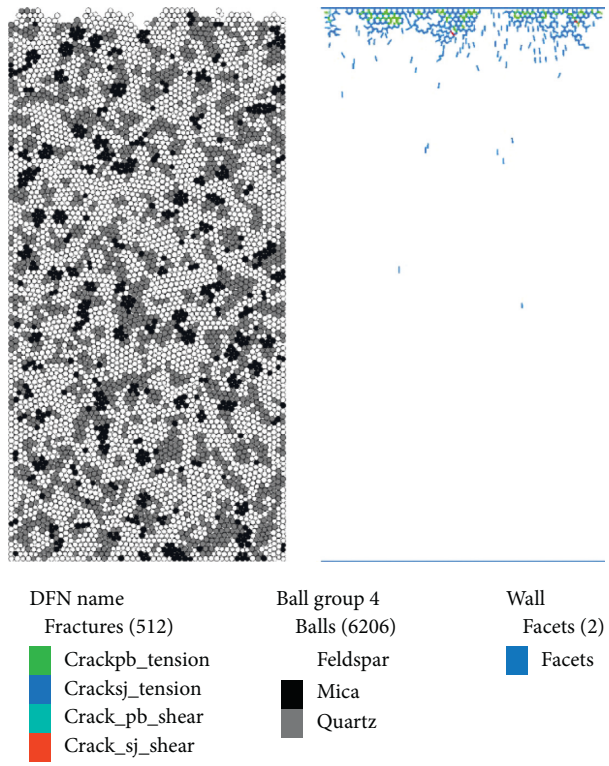

Figure 14: The crack development of rock model under ultrasonic high-frequency excitation.

the modeling process, the parallel bond model is used to simulate the bond mechanics relationship inside the grain. It is known that the smooth joint tensile cracks and the smooth joint shear cracks are distributed at the grain boundaries, while the parallel bond tensile cracks and parallel bond shear cracks are distributed inside the grains.

The variation of the number of different types of cracks in the rock model with time substeps is shown in Figure 15. It is obvious that the number of cracks that are broken by the tension occupies a controlling position. The simulation results show that the mechanism of rock crack propagation under ultrasonic high-frequency excitation is mainly tensile failure. Figure 16 shows the rose diagram of the crack orientation of rock model under ultrasonic vibration, where the direction of 90° is parallel to the direction of ultrasonic vibration loading. According to Figure 16, cracks in rock under ultrasonic vibration tend to propagate parallel to the direction of loading. The simulation results are in good agreement with the experimental results shown in Figure 13.

In addition, the stress wave generated by the ultrasonic vibration is transmitted as a sinusoidal P wave in the granite medium and periodically changes with time. In the time series, the same mass is subjected to compression and tensile periodic loading. The acceleration of the granite can be obtained by deriving formula (2) as follows:

$$a = -A\omega^2 \sin(\omega t). \tag{4}$$

Substitute "$\omega = 2\pi f$" into equation (4):

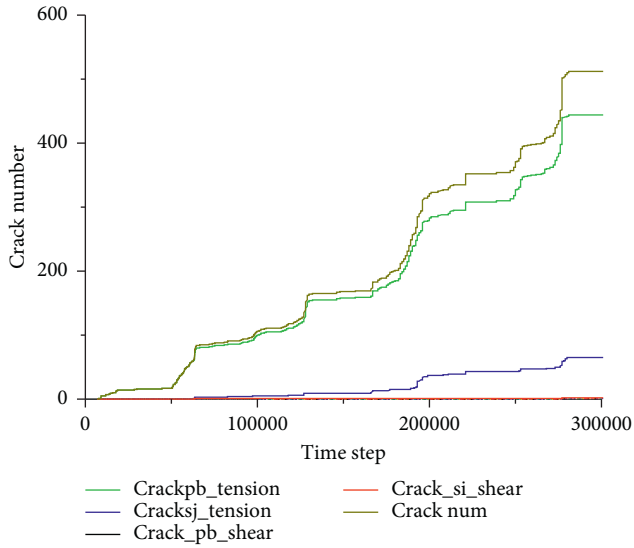

Figure 15: The curve of crack change with time step.

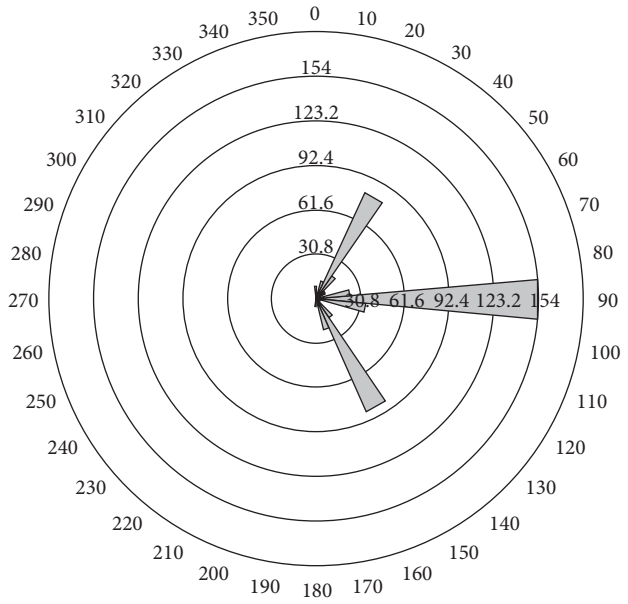

Figure 16: The rose diagram of crack orientation.

$$a = -A4\pi^2 f^2 \sin 2\pi f t. \tag{5}$$

It can be known from formula (5) that the acceleration of the rock is proportional to the square of the ultrasonic vibration frequency. For the internal particle unit of the rock, the force state is as shown in formula (5).

$$F = \Delta m a = -\Delta m A4\pi^2 f^2 \sin 2\pi f t, \tag{6}$$

where Δm is the mass of the particle unit of the granite, A is the maximum stress amplitude generated by the ultrasonic vibration, and f is the frequency of the ultrasonic vibration.

It is known from formula (6) that the force of the internal particle unit of the rock is proportional to the square of the frequency of the ultrasonic vibration. Even if the ultrasonic wave has a small amplitude, it can generate a large excitation force inside the rock due to the high frequency.

The classical fracture mechanics approach considers that the propagation of cracks in the material is highly dependent on the stress intensity. According to the maximum tensile stress theory, when the tensile stress σ_1 at the crack tip exceeds the critical value, the crack begins to propagate [31]. The propagation mechanism of cracks in rock materials under dynamic loading is significantly different from that under static loads. Cracks can grow at a lower cyclic load level compared to the static case. This phenomenon is called subcritical crack propagation and depends on the mechanical behavior of the fracture process zone [32]. This subcritical crack is due to a diffuse microfracturing and decohesion of the rock structure [33]. Erarslan [30] carried out cyclic load tests on tuff plates; it was found that the fracture toughness of rock internal cracks under cyclic loading is reduced by 43% compared to static loads. For the rock under ultrasonic vibration, fatigue damage will occur inside the rock, and the fracture toughness of the crack will decrease. When the exciting force exceeds the bonding force of the weak inner part of the granite, crack propagation occurs, resulting in rock failure.

5. Conclusions

In this paper, the propagation characteristics of cracks in granite under ultrasonic vibration are studied by combining experimental and numerical simulation methods. The growth of microcracks in rock samples after ultrasonic vibration for 0, 2, and 4 minutes was observed by scanning electron microscopy. One heterogeneous granite model was established by using the discrete component software PFC^{2D} to solve the cracking mechanism and orientation of cracks under ultrasonic vibration.

The electron microscope images obtained in the experiment show that the types of cracks which cause the failure of quartz grains are intragranular cracks, transgranular cracks, and grain boundary cracks. The crustal fracture appears in the quartz grains, which shows typical brittle fracture pattern. The types of cracks that cause the failure of feldspar grains are mainly intragranular cracks and transgranular cracks. The growth of microcracks in the feldspar grains shows a wavy pattern. Mica failure is mainly caused by grain boundary crack, and the effect of lamellar cleavage on the failure of mica is significant. The macroscopic morphology of the damaged rock sample shows that the orientation of the macroscopic crack that eventually leads to the failure of the rock sample is parallel to the ultrasonic vibration loading direction.

Numerical simulation results show that there are four cracks in the rock model, including parallel bond tensile cracking cracks (crackpb_tension), smooth joint tensile cracking cracks (cracksj_tension), parallel bond shear cracks (crack_pb_shear), and smooth joint shear cracks (crack_sj_shear), where the number of cracks that are broken by the tension occupies a controlling position. The rose orientation of crack direction shows that the crack tends

to propagate parallel to the loading direction under ultrasonic vibration. It is in good agreement with the experimental results shown in Figure 13.

It is not difficult to find that the ultrasonic high-frequency vibration can effectively promote the germination of new microcracks. The growth and coalescence of the existing microcracks in granite sample will also emerge. These phenomena will lead to the failure of rock sample. The failure of feldspar grains is the main factor to determine the failure of granite when the ultrasonic high-frequency excitation is applied on the granite samples because feldspar grains account for most of the volume fraction (60%–70%). The numerical simulation and theoretical analysis show that the mechanism of crack propagation in rock under ultrasonic vibration is tensile failure.

Data Availability

The data used to support the findings of this study are available from the corresponding author upon request.

Conflicts of Interest

The authors declare that they have no conflicts of interest.

Acknowledgments

The authors thank the National Natural Science Fund Project of China (project name: The Researches on the Mechanism of Broken Rock with Ultrasonic Vibration; project number: 41572356) and Key Lab of Drilling and Exploitation Technology in Complex Conditions, Ministry of Land and Resources, China, for the technical and economic support.

References

[1] P. K. S. C. Fernando, M. Zhang, and Z. Pei, "Rotary ultrasonic machining of rocks: an experimental investigation," *Advances in Mechanical Engineering*, vol. 10, no. 3, article 168781401876317, 2018.

[2] H. Li, D. Yang, Z. Zhong, Y. Sheng, and X. Liu, "Experimental investigation on the micro damage evolution of chemical corroded limestone subjected to cyclic loads," *International Journal of Fatigue*, vol. 113, pp. 23–32, 2018.

[3] N. A. Al-Shayea, "Effects of testing methods and conditions on the elastic properties of limestone rock," *Engineering Geology*, vol. 74, no. 1-2, pp. 139–156, 2004.

[4] S. K. Ray, M. Sarkar, and T. N. Singh, "Effect of cyclic loading and strain rate on the mechanical behaviour of sandstone," *International Journal of Rock Mechanics and Mining Sciences*, vol. 36, no. 4, pp. 543–549, 1998.

[5] M. N. Bagde and V. Petroš, "Fatigue and dynamic energy behaviour of rock subjected to cyclical loading," *International Journal of Rock Mechanics and Mining Sciences*, vol. 46, no. 1, pp. 200–209, 2009.

[6] M. N. Bagde and V. Petroš, "Fatigue properties of intact sandstone samples subjected to dynamic uniaxial cyclical loading," *International Journal of Rock Mechanics and Mining Sciences*, vol. 42, no. 2, pp. 237–250, 2005.

[7] X. S. Liu, J. G. Ning, Y. L. Tan, and Q. H. Gu, "Damage constitutive model based on energy dissipation for intact rock subjected to cyclic loading," *International Journal of Rock Mechanics and Mining Sciences*, vol. 85, pp. 27–32, 2016.

[8] J.-L. Le, J. Manning, and J. F. Labuz, "Scaling of fatigue crack growth in rock," *International Journal of Rock Mechanics and Mining Sciences*, vol. 72, pp. 71–79, 2014.

[9] M. Ghamgosar and N. Erarslan, "Experimental and numerical studies on development of fracture process zone (FPZ) in rocks under cyclic and static loadings," *Rock Mechanics and Rock Engineering*, vol. 49, no. 3, pp. 893–908, 2015.

[10] M. Wiercigroch, J. Wojewoda, and A. M. Krivtsov, "Dynamics of ultrasonic percussive drilling of hard rocks," *Journal of Sound and Vibration*, vol. 280, no. 3–5, pp. 739–757, 2005.

[11] S. Yin, D. Zhao, and G. Zhai, "Investigation into the characteristics of rock damage caused by ultrasonic vibration," *International Journal of Rock Mechanics and Mining Sciences*, vol. 84, pp. 159–164, 2016.

[12] T. Kazerani and J. Zhao, "Micromechanical parameters in bonded particle method for modelling of brittle material failure," *International Journal for Numerical and Analytical Methods in Geomechanics*, vol. 34, no. 18, pp. 1877–1895, 2010.

[13] H. Lee and S. Jeon, "An experimental and numerical study of fracture coalescence in pre-cracked specimens under uniaxial compression," *International Journal of Solids and Structures*, vol. 48, no. 6, pp. 979–999, 2011.

[14] D. M. Ivars, M. E. Pierce, C. Darcel et al., "The synthetic rock mass approach for jointed rock mass modelling," *International Journal of Rock Mechanics and Mining Sciences*, vol. 48, no. 2, pp. 219–244, 2011.

[15] Z. Cui and W. Han, "In situ scanning electron microscope (SEM) observations of damage and crack growth of shale," *Microscopy and Microanalysis*, vol. 24, no. 2, pp. 107–115, 2018.

[16] A. Keneti and B.-A. Sainsbury, "Characterization of strainburst rock fragments under a scanning electron microscope—an illustrative study," *Engineering Geology*, vol. 246, pp. 12–18, 2018.

[17] Q. Liu, Q. Liu, Y. Pan, X. Liu, X. Kong, and P. Deng, "Microcracking mechanism analysis of rock failure in diametral compression tests," *Journal of Materials in Civil Engineering*, vol. 30, no. 6, article 04018082, 2018.

[18] W.-L. Tian, S.-Q. Yang, L.-X. Xie, and Z.-L. Wang, "Cracking behavior of three types granite with different grain size containing two non-coplanar fissures under uniaxial compression," *Archives of Civil and Mechanical Engineering*, vol. 18, no. 4, pp. 1580–1596, 2018.

[19] S.-Q. Yang, W.-L. Tian, and Y.-H. Huang, "Failure mechanical behavior of pre-holed granite specimens after elevated temperature treatment by particle flow code," *Geothermics*, vol. 72, pp. 124–137, 2018.

[20] J. Peng, L. N. Y. Wong, C. I. Teh, and Z. Li, "Modeling microcracking behavior of bukit timah granite using grain-based model," *Rock Mechanics and Rock Engineering*, vol. 51, no. 1, pp. 135–154, 2017.

[21] Y. Shuo et al., "Genesis study on mafic microgranular enclave from early jurassic granites in the southern Zhangguangcai mountains in Heilongjiang province," *Geoscience*, vol. 31, no. 1, pp. 33–45, 2017.

[22] S. Chen, Z. Q. Yue, and L. G. Tham, "Digital image based numerical modeling method for heterogeneous geomaterials," *Chinese Jounal of Geotechnical Engineering*, vol. 27, no. 8, pp. 956–964, 2005.

[23] S. Guangzhong, *Rock Mass Structure Mechanics*, Science Press, Beijing, China, 1988.

[24] W. Gao, L. Wang, and S. He, "Study on rock fracture failure criterion based on energy principles," *Advanced Science Letters*, vol. 4, no. 3, pp. 869–874, 2011.
[25] S. Cowie and G. Walton, "The effect of mineralogical parameters on the mechanical properties of granitic rocks," *Engineering Geology*, vol. 240, pp. 204–225, 2018.
[26] Ö. Ündül, F. Amann, N. Aysal, and M. L. Plötze, "Microtextural effects on crack initiation and crack propagation of andesitic rocks," *Engineering Geology*, vol. 193, pp. 267–275, 2015.
[27] F. Amann, Ö. Ündül, and P. K. Kaiser, "Crack initiation and crack propagation in heterogeneous sulfate-rich clay rocks," *Rock Mechanics and Rock Engineering*, vol. 47, no. 5, pp. 1849–1865, 2013.
[28] G. Swan, "Fracture stress scale effects for rocks in bending," *International Journal of Rock Mechanics and Mining Sciences & Geomechanics Abstracts*, vol. 17, no. 6, pp. 317–324, 1980.
[29] Y. Kudo, K. I. Hashimoto, O. Sano, and K. Nakagawa, "Relation between physical anisotropy and microstructures of granitic rock in Japan," in *Poceedings of the 6th International Congress on Rock Mechanics*, pp. 429–432, Montreal, Canada, August–September 1987.
[30] N. Erarslan, "Microstructural investigation of subcritical crack propagation and fracture process zone (FPZ) by the reduction of rock fracture toughness under cyclic loading," *Engineering Geology*, vol. 208, pp. 181–190, 2016.
[31] A. Manouchehrian and M. F. Marji, "Numerical analysis of confinement effect on crack propagation mechanism from a flaw in a pre-cracked rock under compression," *Acta Mechanica Sinica*, vol. 28, no. 5, pp. 1389–1397, 2012.
[32] F. Barpi and S. Valente, "Subcritical crack propagation under cyclic load of concrete structures," *Magazine of Concrete Research*, vol. 62, no. 7, pp. 489–496, 2010.
[33] B. Cerfontaine and F. Collin, "Cyclic and fatigue behaviour of rock materials: review, interpretation and research perspectives," *Rock Mechanics and Rock Engineering*, vol. 51, no. 2, pp. 391–414, 2017.